Electronic Journal of Biotechnology 50 (2021) 10–15

Contents lists available at ScienceDirect

Electronic Journal of Biotechnology

journal homepage:

Research Article

# LXYL-P1-2 immobilized on magnetic nanoparticles and its potential application in paclitaxel production

Sen Zou [a,c,1], Tian-Jiao Chen [b,1], Dan-Yang Li [a], Shuai Fan [a], Zhao-Yong Yang [a,*], Ping Zhu [b,*]

[a] Key Laboratory of Biotechnology of Antibiotics, Institute of Medicinal Biotechnology, Chinese Academy of Medical Sciences & Peking Union Medical College, Beijing 100050, China
[b] State Key Laboratory of Bioactive Substance and Function of Natural Medicines & NHC Key Laboratory of Biosynthesis of Natural Products, Institute of Materia Medica, Chinese Academy of Medical Sciences & Peking Union Medical College, Beijing 100050, China
[c] Research Center, The First Affiliated Hospital of Zhengzhou University, Zhengzhou, 450052 Henan, China

ARTICLE INFO

*Article history:*
Received 4 May 2020
Accepted 22 December 2020
Available online 31 December 2020

*Keywords:*
10-Deacetyltaxol
7-β-Xylosyltaxane glycoside hydrolases
Enzyme kinetics
Glycoside hydrolase
Immobilization
Industrial production
Magnetic nanoparticles
Paclitaxel
Reusability

ABSTRACT

*Background:* LXYL-P1-2 is the first reported glycoside hydrolase that can catalyze the transformation of 7-β-xylosyl-10-deacetyltaxol (XDT) to 10-deacetyltaxol (DT) by removing the D-xylosyl group at the C-7 position. Successful synthesis of paclitaxel by one-pot method combining the LXYL-P1-2 and 10-deacetylbaccatin III-10-β-*O*-acetyltransferase (DBAT) using XDT as a precursor, making LXYL-P1-2 a highly promising enzyme for the industrial production of paclitaxel. The aim of this study was to investigate the catalytic potential of LXYL-P1-2 stabilized on magnetic nanoparticles, the surface of which was modified by $Ni^{2+}$-immobilized cross-linked $Fe_3O_4$@Histidine.

*Results:* The diameter of matrix was 20–40 nm. The $K_m$ value of the immobilized LXYL-P1-2 catalyzing XDT (0.145 mM) was lower than that of the free enzyme (0.452 mM), and the $k_{cat}/K_m$ value of immobilized enzyme (12.952 mM $s^{-1}$) was higher than the free form (8.622 mM $s^{-1}$). The immobilized form maintained 50% of its original activity after 15 cycles of reuse. In addition, the stability of immobilized LXYL-P1-2, maintained 84.67% of its initial activity, improved in comparison with free form after 30 d storage at 4°C.

*Conclusions:* This investigation not only provides an effective procedure for biocatalytic production of DT, but also gives an insight into the application of magnetic material immobilization technology.

**How to cite**: Zou S, Chen TJ, Li DY, et al. LXYL-P1-2 immobilized on magnetic nanoparticles and its potential application in paclitaxel production. Electron J Biotechnol 2021;50.https://doi.org/10.1016/j.ejbt.2020.12.005



## 1. Introduction

LXYL-P1-2, which is a β-xylosidase/β-glucosidase bifunctional enzyme obtained from *Lentinula edodes*, can specifically hydrolyze the xylosyl group of 7-β-xylosyl-10-deacetyltaxol (XDT) to form 10-deacetyltaxol (DT), which, in turn, can be used as a precursor to synthesize paclitaxel by only one step of enzymatic acetylation [1,2]. Paclitaxel (Taxol®) is one of the best natural anti-cancer drugs ever found, currently approved for the treatment of breast cancer [3], ovarian cancer [4], prostate cancer [5], non-small cell lung cancer [6], small cell lung cancer [7], etc. Paclitaxel was initially isolated from the bark of *Taxus brevifolia* which grows extremely slowly [8]. The supply source of paclitaxel has always been a top concern because its content in the plant is extremely low (the highest content is only about 0.02% which is from the bark of the trees) [9]. In order to overcome the current insufficiency of paclitaxel, a one-pot reaction system based on XDT (the analog of paclitaxel) and the combination of two steps of enzymatic synthesis has been successfully established [2]. LXYL-P1-2 is responsible for catalyzing the first step of the reaction. In previous studies, we showed that LXYL-P1-2 had good stability during the reaction [1]. If the enzyme can be reused, the cost of paclitaxel production will be greatly reduced.

Immobilizing enzymes on artificially fabricated carriers for their efficient use and easy removal from reactants has attracted enormous interest for decades [10]. There are different immobilizing ways according to the different types of carrier materials, such as natural polymers (including chitosan, cellulose) [11], synthetic

Peer review under responsibility of Pontificia Universidad Católica de Valparaíso
* Corresponding authors.
*E-mail addresses:* zhaoyongy@imb.pumc.edu.cn (Z.-Y. Yang), zhuping@imm.ac.cn (P. Zhu).
[1] These authors contributed equally to this work.

https://doi.org/10.1016/j.ejbt.2020.12.005

polymers [12], magnetic nanomaterials [13], mesoporous material [14]. Although natural polymers were widely sourced and of low cost, they have low mechanical strength and are easily decomposed by microorganisms. As to synthetic polymers, the combination of synthetic polymers and enzyme molecules is not stable enough and easy to be apart off, and the polymer material has cytotoxicity and poor biocompatibility, causing limitation in practical applications. Magnetic nanomaterials and mesoporous materials, as immobilized materials, have been highly studied. Magnetic nanomaterials can change the motion of the particle by changing the magnetic force strength and the direction of the external magnetic field, so the combination and separation of enzyme and carrier can be completely under control, shedding light on the separation and reuse of immobilized enzyme [15]. Furthermore, there appeared novel magnetic nanomaterials composed of a high-magnetic-response supra-particle ($Fe_3O_4$) core and a $Ni^{2+}$-immobilized material, like polyvinyl imidazole (PVIM), iminodiacetic acid (IDA), and silicate, in which the $Ni^{2+}$-immobilized material could effectively immobilize His-tagged enzymes [16,17,18]. Magnetic composite microspheres have been extensively investigated owing to their excellent magnetic responsiveness and their application in protein immobilization [15]. $Fe_3O_4$@Histidine-Ni magnetic nanoparticle have the advantages of large surface area, easy surface modification, and high stability in various pH and temperatures. Most important of all, it can immobilize His-tagged enzymes by metal-ion affinity without reducing enzyme catalytic activity [16]. The immobilized enzymes, such as bacterial cellulase, *Bacillus* sp. laccase and *Chlorella vulgaris* exopolysaccharides, showing enhanced stability, activity, and other promising application characteristics [19,20,21]. Compared with other materials, immobilized LXYL-P1-2 on magnetic materials was more easily and faster separated from substrates and products by magnetic force. Magnetic materials could be recycled by affinity combination and dissociation with His-tag of enzymes.

In the present study, immobilization of LXYL-P1-2 onto $Fe_3O_4$@-Histidine-Ni magnetic nanoparticles was implemented with the aim to improve the utilization efficiency of the enzyme. The particle size, optimum temperature and pH, reusability, and storage ability of the immobilized LXYL-P1-2 were studied. The enzymatic reaction kinetics of the free and the immobilized LXYL-P1-2 were also investigated. The kinetic parameters were calculated with the Michaelis–Menten equation. By immobilized with the magnetic materials containing His-tag binding region, the catalytic efficiency onto XDT, acid tolerance, and enzyme utilization efficiency of LXYL-P1-2 were significantly improved in comparison with the free form. This study provides a prerequisite for further optimization of the paclitaxel synthesis based on magnetic immobilization.

## 2. Materials and methods

### 2.1. Substrates and chemicals

XDT used in this study was purchased from Fujian South Pharmaceutical Co., Ltd, (Fujian, China) and then fully purified by medium pressure liquid chromatography (MPLC) method (LC2000, equipped with ultraviolet detector, Separation technology Co., Ltd, Beijing, China) established in the previous study [1]. All other chemicals were analytical grade unless otherwise indicated.

### 2.2. Protein expression and purification

The engineered strain GS115-3.5K-P1-2 was constructed and incubated as before [1]. Enzyme purification was also followed in the previous study [22].

### 2.3. Immobilization

$Fe_3O_4$@Histidine-Ni magnetic nanoparticles matrix was synthesized as described previously [23]. A matrix of 50 mg was washed three times using 20 mM Tris-HCl buffer (pH 8.0), and 2 mg/mL LXYL-P1-2 protein was added to matrix and incubated overnight. Magnet was used to separate immobilized enzyme from protein buffer as demonstration (Fig. 1). The amount of binding protein was calculated with the following equation:

$$\text{Amount of binding protein} = \frac{\text{Amount of protein added-Amount of protein remained}}{\text{Amount of protein added}}$$

Protein concentration was measured with Bradford assay. The morphology and size of the particles were analyzed using a field emission scanning electron microscope (Hitachi SU8010).

### 2.4. Characterization of the immobilized LXYL-P1-2

Characterization analysis of the immobilized LXYL-P1-2 on XDT was conducted in a total reaction system of 300 μL, containing 100 μL 0.01 mg/mL immobilized protein in 20 mM Tris-HCl buffer (pH 8.0) and 200 μL 2 mg/mL XDT, incubated at 800 rpm for 90 min. To measure the optimal pH, 100 mg/mL XDT (dissolved in 100% DMSO) was diluted in 50 mM sodium acetate buffer with pH 3.0–5.5, or in 50 mM sodium phosphate buffer with pH 6.0–9.0 to 2 mg/mL, and then added to the system above. The reaction was performed under 800 rpm for 90 min at 45°C. To measure the optimal temperature, XDT was diluted to 2 mg/mL in 50 mM sodium acetate buffer with pH 4.0 constantly, and the reaction was conducted at a temperature range of 25–65°C under 800 rpm for 90 min. The time curves of the immobilized enzyme against XDT were also determined under pH 4.0 at 35°C and 45°C, respectively. Reactions were stopped by adding 700 μL methyl alcohol into each reaction solution, and the mixtures were analyzed via HPLC. Each datum was measured in triplicates. The standard curves and linear regression equations of DT as well as the HPLC detection conditions were as described previously [1]. The highest activity was considered as 100%, and the activity of remaining points was expressed as a percentage of the highest activity.

Fourier transform infrared spectroscopy (FTIR) spectra was measured using VERTEX 70V (Bruker) in the range from 500 to 4000 $cm^{-1}$. X-ray diffraction (XRD) measurements were employed on D8 Discover diffractometer (Bruker) at a scanning speed of 4°/min in the $2\theta$ range from 10° to 90° with Cu-K radiation ($\lambda$ = 0.154056 nm).

### 2.5. Kinetics of the free and the immobilized LXYL-P1-2

The kinetic parameters of the free and the immobilized enzyme were determined against XDT in a concentration range of 0.039–5 mg/ml in the aforementioned total system and at each optimum condition for 1 h. Data were fitted to the Linewear–Burk plot and

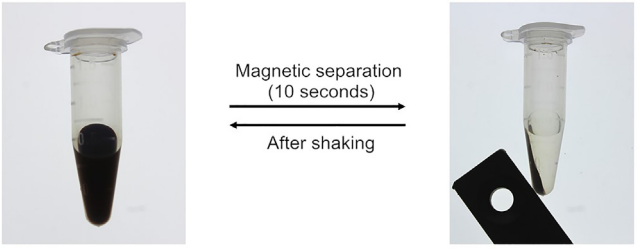


**Fig 1.** Magnetic separation during immobilization.

$K_m$ and $V_{max}$ were extrapolated from the slope and the intercept, respectively, using the Michaelis–Menten equation:

$$\frac{1}{V} = \frac{K_m}{V_{max}}\left[\frac{1}{S}\right] + \left[\frac{1}{V_{max}}\right]$$

When the LXYL-P1-2 was saturated with the XDT substrate, the catalytic reaction reached the maximum reaction rate ($V_{max}$). The $k_{cat}$ value can be calculated by the formula $k_{cat} = V_{max}/E_t$. $E_t$ represented the molar concentration of LXYL-P1-2 in the reaction system. The MS detection showed that the molecular weight of LXYL-P1-2 is 120 kDa [1].

### 2.6. Reusability and storage stability

The reusability was determined by measuring the activity of immobilized enzyme in nineteen cycles of use. In each cycle, magnetic nanoparticles matrix containing 0.5 mg immobilized enzyme was mixed with 6 mL 0.25 mg/mL XDT in 50 mM sodium acetate buffer (pH 4.0) and incubated at 35°C for 1 h under 200 rpm shaking. Magnet was used to separate the enzyme from the reaction mixture and a 300 μL separated reaction supernatant was taken and mixed with 700 μL methyl alcohol for HPLC analysis. The matrix was washed with 6 mL 20 mM Tris-HCl buffer (pH 8.0) on ice before the next cycle. The initial activity was considered as 100%, and the activity of the remaining cycles was expressed as a percentage of the initial one.

The storage stability of the free and immobilized LXYL-P1-2 was determined by measuring the released *p*-nitrophenol from PNP-Xyl (*p*-nitrophenyl-*β*-D-xylopyranoside) at fixed intervals from stored in pH 8.0 buffer media at 4°C for 30 d as described previously [1]. The pH and temperature stability were determined in similar ways after stored in pH 4.5 buffer media (optimal pH) at 25°C (room temperature) and pH 8.0 buffer media at 45°C (optimal temperature), respectively. The sampling interval for pH and temperature stability detection was set to 30 min. The enzyme activity on the first day was considered as 100%, and activity of the remaining times was expressed as a percentage of the initial one.

## 3. Results and discussion

### 3.1. LXYL-P1-2 immobilization

In the previous study [1], novel gene (*lxyl-p1-2*) has been obtained from *L. edodes* and heterologously expressed in *Pichia pastoris* GS115 strain. The recombinant protein has been proved to specifically hydrolyze xylose from XDT. Herein, we try to find a suitable way to immobilize the enzyme to increase its potential for industry application. In this article, $Fe_3O_4$@Histidine-Ni magnetic nanoparticles matrix has a good performance in binding proteins. The immobilization quantity of LXYL-P1-2 on $Fe_3O_4$@Histidine-Ni magnetic nanoparticles matrix is up to 76 μg/mg after overnight immobilization, similar to the binding amount of magnetic composite microspheres which has been reported [18] and much higher than other materials. For example, the binding amount of lipase to γ-$Fe_2O_3$ magnetic nanoparticles was 55.6 μg/mg [24], immobilization amount of diastase α-amylase on nano zinc oxide was 6.6 μg/mg [25], Penicillin G acylase (PGA) was immobilized on magnetic $Fe_3O_4$@chitosan nanoparticles at a concentration of 8.8 μg/mg [26], and immobilization amount of lignin peroxidase on spherical mesoporous material was 8.87 μg/mg [27]. SEM was used to determine the size and morphology of magnetic nanoparticles. As can be seen in the Fig. 2, particles are spherical and have a mean diameter of 20–40 nm in the range of nanometers. Comparing the images of $Fe_3O_4$@Histidine-Ni and $Fe_3O_4$@-Histidine-Ni/LXYL-P1-2, there was no significant change in the shape and size of particles after enzyme immobilization. Larger specific surface to volume ratio of the small dimensions provided higher efficient enzyme immobilization.

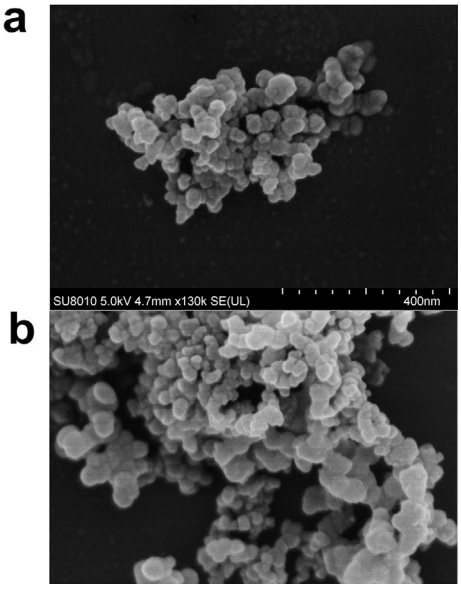


**Fig 2.** SEM images of $Fe_3O_4$@Histidine-Ni magnetic nanoparticles. (a) $Fe_3O_4$@-Histidine-Ni. (b) $Fe_3O_4$@Histidine-Ni/LXYL-P1-2.

### 3.2. Characterization of the free and the immobilized LXYL-P1-2

Since $Fe_3O_4$@Histidine-Ni magnetic nanoparticles matrix was easy to precipitate, the reaction of the $Fe_3O_4$@Histidine-Ni/LXYL-P1-2 with XDT was carried out at 800 rpm after the test. The optimum pH of the immobilized LXYL-P1-2 against XDT was found to be pH 4.0, which is more acidic than the optimum pH 4.5 of the free enzyme [1] as shown in Fig. 3a. Furthermore, the immobilized LXYL-P1-2 showed a better stability under acidic conditions, since the activity of the immobilized enzyme at pH 3.0 was maintained by 88% of the optimum conditions, whereas the free enzyme maintained only 17% of the highest activity at the same pH (Fig. 3a).

The optimal temperature for the immobilized enzyme against XDT was found to be around 45°C, quite similar to that for the free enzyme [1]. But at 50°C and 55°C, the immobilized enzyme both remained much higher activities than the free enzyme, showing an increased temperature tolerance of the immobilized LXYL-P1-2 (Fig. 3b). This may be due to the covalent bond between the enzyme and supports, which is capable of increasing the conformational rigidity of the enzyme and the activation energy of the thermal denaturation reaction [28].

It is known that an enzyme has a trade-off between stability and activity leading to an impossible mission of optimizing performance at both high and low temperatures [29]. With the increase of reaction temperature, enzymatic activity usually declines sharply because the stability of the enzyme structure is destroyed at high temperature. The reaction temperature is usually lowered in industrial production to enhance stability for longer time use [30]. Here, we compared the XDT conversion by the immobilized LXYL-P1-2 at the optimum temperature and 35°C (which is 10°C lower than the optimum temperature). As shown in Fig. 3c, we found that although the XDT conversion rate of the immobilized LXYL-P1-2 at 45°C was more than twice that at 35°C within the first 0.5 h, the difference in conversion rate was reduced to about 1.5 times after 1 h of reaction between two temperatures. During the next few hours of reaction, the difference in XDT conversion

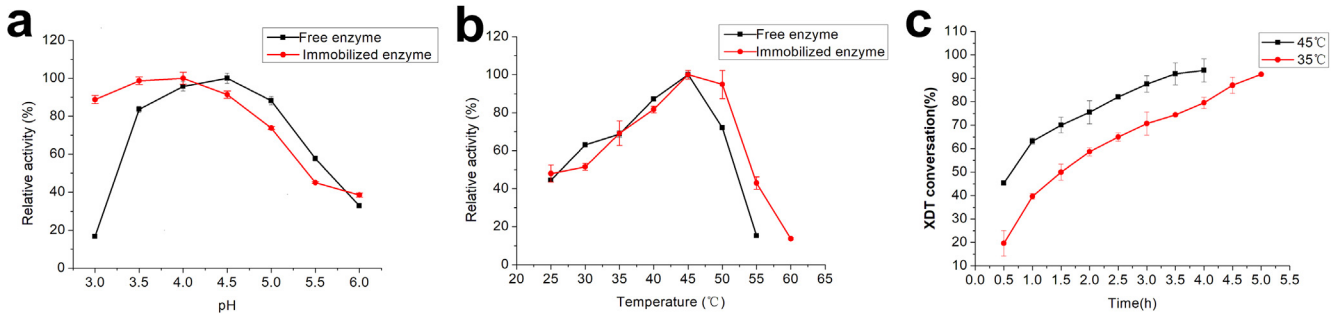


**Fig 3.** Characterization of the free [1] and the immobilized LXYL-P1-2. (a) Effects of pH on activity against XDT. (b) Effects of temperature on activity against XDT. (c) XDT conversation (%) under 35°C and 45°C.

rate at the two temperatures was further reduced, eventually both reaching more than 90%, with only one-hour difference between them.

Fourier transform infrared spectroscopy (FTIR) and X-ray diffraction (XRD) were employed to evaluate the characterization of the $Fe_3O_4$@Histidine-Ni and $Fe_3O_4$@Histidine-Ni/LXYL-P1-2. FTIR spectra of $Fe_3O_4$@Histidine-Ni have been shown in Fig. 4a, and the absorption peak at 589 $cm^{-1}$ was assigned to Fe–O bond vibration. The obvious peak at 1079 $cm^{-1}$ was attributed to C–O stretching vibration. Signals related to the vibrations of carboxylic and hydroxyl groups were located at 1631 $cm^{-1}$ and 3423 $cm^{-1}$, respectively [23]. The XRD spectra of $Fe_3O_4$@Histidine-Ni and $Fe_3O_4$@Histidine-Ni/LXYL-P1-2 are compared in Fig. 4b. Six typical peaks of $Fe_3O_4$@-Histidine-Ni ($2\theta$ = 30.1°, 35.7°, 43.3°, 53.6°, 57.2°, and 63.0°) were observed, which corresponding to the (220), (311), (400), (422), (511), and (440) lattice planes of standard $Fe_3O_4$ (JCPDS 19-0629) [31]. Overall, immobilization of LXYL-P1-2 onto $Fe_3O_4$@Histidine-Ni did not significantly change the number, position, and intensity of the peaks in FTIR/XRD spectra, indicating that the LXYL-P1-2 does not change the main structure of $Fe_3O_4$@Histidine-Ni magnetic nanoparticles.

### 3.3. Kinetics of the free and immobilized LXYL-P1-2

The changes in enzymatic kinetic parameters after immobilization could be monitored to reflect the success of immobilization. The kinetic parameters of the free and immobilized LXYL-P1-2 with XDT were determined, and the results are listed in Table 1. The $K_m$ of the free LXYL-P1-2 was 3-fold higher than that of the immobilized one, indicating that the affinity of LXYL-P1-2 to the substrate XDT was significantly increased after immobilization. Although the $V_{max}$ and $k_{cat}$ of the immobilized enzyme were both lower than that of the free one, the $k_{cat}/K_m$ of immobilized enzyme against XDT was about 1.5-fold higher than that of the free enzyme due to the decreased $K_m$ value, demonstrating the improved catalytic efficiency of the immobilized enzyme. Similar results were observed by Klapiszewski et al. [32] who found a decrease in $V_{max}$ and an increase in $K_m$ for alpha-amylase immobilized on a titania/lignin novel hybrid support. The decreased $K_m$ value of the immobilized enzyme is related to the charge on the substrate and/or carrier, diffusion effects, and, in some cases, three-dimensional structure changes in enzyme configuration.

### 3.4. Reusability and storage stability of immobilized LXYL-P1-2

The reusability and storage stability of immobilized enzymes were the main concerns that can limit the industrial implementation of any immobilized enzymes. The main advantages of immobilization are easy to separate and reuse. To increase enzyme stability and simplify production process, we evaluated the reusability of immobilized LXYL-P1-2 by measuring the catalytic activity at optimum pH but at a temperature of 35°C at intervals of 1 h. The first run was a control and its specific activity was set to 100%. The results are depicted in Fig. 5a. Immobilized enzyme was recycled for 19 consecutive batches, and it kept stable over 15 cycles with a conversion rate of 50%. The loss in activity was attributed to inactivation of enzyme or releases of enzyme from the supports due to its continuous use. Furthermore, the recurrent encountering of substrate with the active site of immobilized enzyme may cause distortion and lead to loss of activity. Similarly,

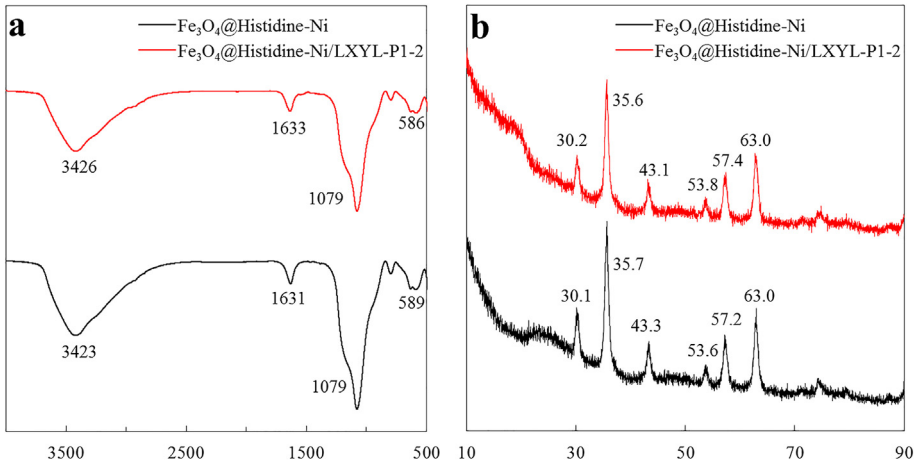


**Fig 4.** FTIR (a) and XRD (b) spectra of $Fe_3O_4$@Histidine-Ni and $Fe_3O_4$@Histidine-Ni/LXYL-P1-2.

**Table 1**
Kinetic parameters for the hydrolysis of XDT by the free and the immobilized LXYL-P1-2.

| Enzyme form | $V_{max}$ (μM $min^{-1}$) | $K_m$ (mM) | $k_{cat}$ ($s^{-1}$) | $k_{cat}/K_m$ ($s^{-1}$ $mM^{-1}$) |
|---|---|---|---|---|
| Free | 6.780 ± 0.232 | 0.452 ± 0.028 | 3.897 ± 0.133 | 8.622 ± 0.242 |
| Immobilized | 3.268 ± 0.290 | 0.145 ± 0.034 | 1.878 ± 0.167 | 12.952 ± 2.33 |

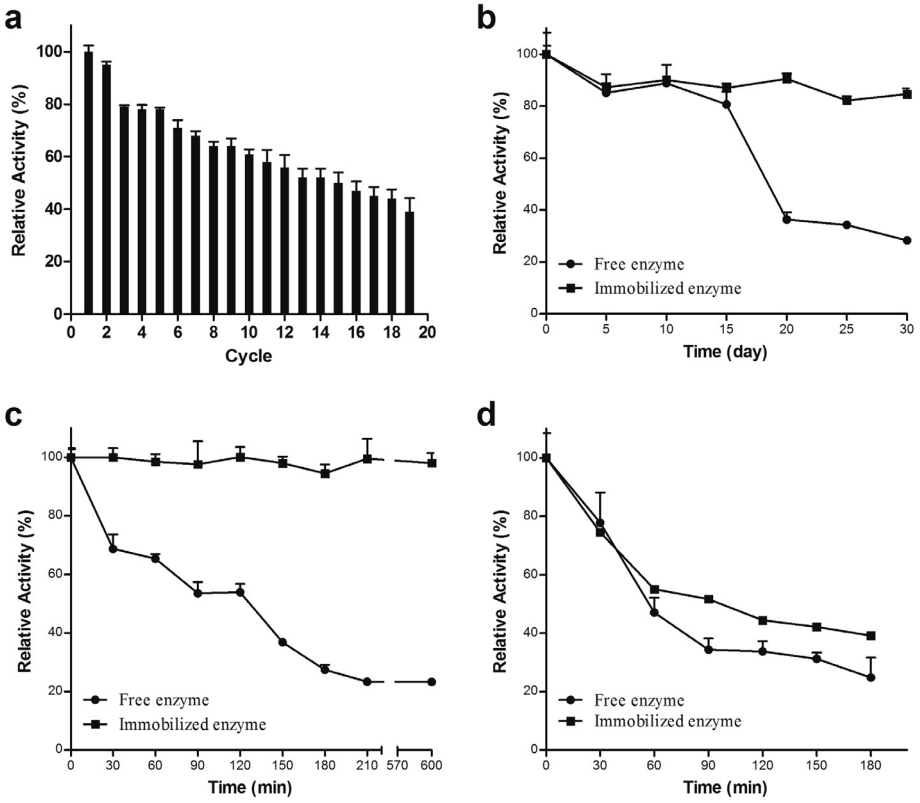


**Fig 5.** (a) Reusability, (b) storage stability (4 °C, pH 8.0), (c) pH stability (25 °C, pH 4.5) and (d) temperature stability (45 °C, pH 8.0) of immobilized LXYL-P1-2.

in another study, xylanase immobilized on magnetic nanoparticles supported hyperbranched polyglycerol (MNP/HPG) and a derivative conjugated with citric acid (MNP/HPG-CA) could retain around 66% and 54% of its initial activity after 10 cycles of reuse, respectively [33]. After LXYL-P1-2 denature, enzyme can be removed by adding high-level imidazole, and the matrix can be used to immobilize new enzyme again. The reuse of enzyme after immobilization makes LXYL-P1-2 more efficient, enhancing its potential to catalyze XDT to DT and making it feasible for the industrial application of paclitaxel production.

The storage stability of free and immobilized enzyme was studied for 30 d. As presented in Fig. 5b, the immobilized LXYL-P1-2 was stable for 30 d, retaining 84.67% of its maximum activity, while the free form only retained 28.36% of initial activity. The stability of free LXYL-P1-2 shown in this paper was in accordance with our earlier report [1]. Similar observations were made by Zhang et al., [34] who observed the stability of immobilized alpha-amylase improved in comparison with free form and maintained over 70% after 20 d storage at 4°C. Furthermore, the immobilized LXYL-P1-2 retained >95% of its activity after storing for 10 h in pH 4.5 buffer media at room temperature, while the activity of the free form was only 23% over the same period (Fig. 5c). These findings indicated once again that immobilized LXYL-P1-2 presented better stability under acidic conditions compared to free form. However, both immobilized and free LXYL-P1-2 showed marked decrease in activity after storing at 45°C, and there was no significant difference in the activity of the enzymes (Fig. 5d). These data suggested that immobilization of LXYL-P1-2 onto $Fe_3O_4$@Histidine-Ni magnetic nanoparticles was beneficial to strengthen the stability of LXYL-P1-2, which may be due to the enhancement of the structural rigidity of the enzyme molecule [34].

## 4. Conclusion

LXYL-P1-2 catalyzes 7-β-xylosyl-10-deacetyltaxol by removing 7-β-xylosyl to generate 10-deacetyltaxol, and the product can be used for chemical semisynthesis or biological enzyme catalysis to produce paclitaxel. The discovery of LXYL-P1-2 and its application in the double-enzyme one-pot reaction system will incredibly improve resource utilization, using the analog of paclitaxel from phytochemical extraction, and increase the yield of the final product. The essential purpose of this study was to immobilize LXYL-P1-2 onto $Fe_3O_4$@Histidine-Ni beads to evaluate the potential for industry applications. As for the properties of LXYL-P1-2 enzyme, the optimum temperature was 45°C, and the optimum pH for immobilized enzyme was decreased by about 0.5 units. Compared to free enzyme, immobilized LXYL-P1-2 showed higher environmental tolerance (temperature and pH). The $k_{cat}/K_m$ value of immobilized enzyme was 1.5 higher than that of free enzyme, revealing

the enhancement of the substrate affinity after immobilization. Notably, the reusability experiment showed that immobilized LXYL-P1-2 could be repeatedly used for 15 times with remaining 50% catalytic activity and the requirement of high strict preservation conditions on immobilized LXYL-P1-2 was significantly reduced in comparison with the free form. Overall, this study explored the magnetic immobilization of LXYL-P1-2 for the transformation of XDT to DT, providing promises for the industrial application of paclitaxel production.

## Conflict of interest

The authors declare that they have no conflict of interest.

## Financial support

This work was supported by the National Key Research and Development Program of China (2018YFA0901800, 2018YFA0901900), National Natural Science Foundation of China (81761128016, 81872782, 81573325) and the Drug Innovation Major Project of China (2018ZX09711001-006).

## Acknowledgements

We thank Dr. Guangteng Wu (ArNuXon Pharm-Sci Co., Ltd., Beijing) for the manuscript revision.

## References

[1] Cheng HL, Zhao RY, Chen TJ, et al. Cloning and characterization of the glycoside hydrolases that remove xylosyl groups from 7-β-xylosyl-10-deacetyltaxol and its analogues. Mol Cell Proteomics 2013;12(8):2236–48. https://doi.org/10.1074/mcp.M113.030619. PMid: 23665501.

[2] Li BJ, Wang H, Gong T, et al. Improving 10-deacetylbaccatin III-10-β-O-acetyltransferase catalytic fitness for Taxol production. Nat Commun 2017;8(1):1–14. https://doi.org/10.1038/ncomms15544. PMid: 28516951.

[3] Holmes FA, Walters RS, Theriault RL, et al. Phase II trial of taxol, an active drug in the treatment of metastatic breast cancer. J Natl Cancer Inst 1991;83(24):1797–805. https://doi.org/10.1093/jnci/83.24.1797-a. PMid: 1683908.

[4] Huizing MT, Keung AC, Rosing H, et al. Pharmacokinetics of paclitaxel and metabolites in a randomized comparative study in platinum-pretreated ovarian cancer patients. J Clin Oncol 1993;11(11):2127–35. https://doi.org/10.1200/JCO.1993.11.11.2127. PMid: 7901342.

[5] Roth BJ, Loehrer PJ, Yeap BY, et al. Taxol in advanced, hormone-refractory carcinoma of the prostate. A phase II trial of the eastern cooperative oncology group. Cancer 1993;72(8):2457–60. https://doi.org/10.1002/1097-0142(19931015)72:8<2457::AID-CNCR2820720825>3.0.CO;2-Z. PMid: 8104680.

[6] Kelly RJ, Thomas A, Rajan A, et al. A phase I/II study of sepantronium bromide (YM155, survivin suppressor) with paclitaxel and carboplatin in patients with advanced non-small-cell lung cancer. Ann Oncol 2013;24(10):2601–6. https://doi.org/10.1093/annonc/mdt249. PMid: 23857959.

[7] Ettinger DS, Finkelstein DM, Sarma RP, et al. Phase II study of paclitaxel in patients with extensive-disease small-cell lung cancer: an Eastern Cooperative Oncology Group study. J Clin Oncol 1995;13(6):1430–5. https://doi.org/10.1200/JCO.1995.13.6.1430. PMid: 7751889.

[8] Cragg GM. Paclitaxel (Taxol®): a success story with valuable lessons for natural product drug discovery and development. Med Res Rev 1998;18(5):315–31. https://doi.org/10.1002/(SICI)1098-1128(199809)18:5<315::AID-MED3>3.0.CO;2-W. PMid: 9735872.

[9] Chattopadhyay SK, Sharma RP, Kumar S. Process for the production of taxol analogues 10-deacetyl taxol A, B, and C. European Patent Office Publ. of Application with search report EP19990301915. 11 Mar 1999. [Cited on February 22, 2000]. https://europepmc.org/article/PAT/EP1028116.

[10] Sirisha VL, Jain A, Jain A. Enzyme immobilization: an overview on methods, support material, and applications of immobilized enzymes. Adv Food Nutr Res 2016;79(7):179–211. https://doi.org/10.1016/bs.afnr.2016.07.004. PMid: 27770861.

[11] Homaei A. Enhanced activity and stability of papain immobilized on CNBr-activated sepharose. Int J Biol Macromol 2015;75(1):373–7. https://doi.org/10.1016/j.ijbiomac.2015.01.0559. PMid: 2566187.

[12] Bayramoglu G, Senkal BF, Yilmaz M, et al. Immobilization and stabilization of papain on poly (hydroxyethyl methacrylate–ethylenglycol dimethacrylate) beads grafted with epoxy functional polymer chains via surface-initiated-atom transfer radical polymerization (SI-ATRP). Bioresour Technol 2011;102(21):9833–7. https://doi.org/10.1016/j.biortech.2011.08.042. PMid: 21908189.

[13] Ulu A, Noma AA, Koytepe S, et al. Chloro-modified magnetic $Fe_3O_4$@ MCM-41 core–shell nanoparticles for L-asparaginase immobilization with improved catalytic activity, reusability, and storage stability. Appl Biochem Biotechnol 2019;187(3):938–56. https://doi.org/10.1007/s12010-018-2853-9. PMid: 30101367.

[14] Wu L, Liu Y, Chi B, et al. An innovative method for immobilizing sucrose isomerase on ε-poly-L-lysine modified mesoporous $TiO_2$. Food Chem 2015;187(4):182–8. https://doi.org/10.1016/j.foodchem.2015.04.072. PMid: 25977014.

[15] Tao D, Xuya Y, Junwei X. Research progress of magnetic polymer microspheres immobilized lipase. New Chem Mater 2013;41(11):4–6.

[16] Zhang Y, Li D, Yu M, et al. $Fe_3O_4$/PVIM-$Ni^{2+}$ magnetic composite microspheres for highly specific separation of histidine-rich proteins. ACS Appl Mater Interfaces 2014;6(11):8836–44. https://doi.org/10.1021/am501626t. PMid: 24766586.

[17] Zhang Y, Yang Y, Ma W, et al. Uniform magnetic core/shell microspheres functionalized with $Ni^{2+}$–iminodiacetic acid for one step purification and immobilization of his-tagged enzymes. ACS Appl Mater Interfaces 2013;5(7):2626–33. https://doi.org/10.1021/am4006786. PMid: 23470159.

[18] Shin MK, Kang B, Yoon NK, et al. Synthesis of $Fe_3O_4$@ nickel–silicate core–shell nanoparticles for His-tagged enzyme immobilizing agents. Nanotechnology 2016;27(49):. https://doi.org/10.1088/0957-4484/27/49/495705. PMid: 27831938495705.

[19] Selvam K, Govarthanan M, Senbagam D, et al. Activity and stability of bacterial cellulase immobilized on magnetic nanoparticles. Chin J Catal 2016;37(11):1891–8. https://doi.org/10.1016/S1872-2067(16)62487-7.

[20] Srinivasan P, Selvankumar T, Paray BA, et al. Chlorpyrifos degradation efficiency of Bacillus sp. laccase immobilized on iron magnetic nanoparticles. 3 Biotech 2020;10(366):1–11. https://doi.org/10.1007/s13205-020-02363-6.

[21] Muthusamy G, Jeon CH, Jeon YH, et al. Non-toxic nano approach for wastewater treatment using Chlorella vulgaris exopolysaccharides immobilized in iron-magnetic nanoparticles. Int J Biol Macromol 2020;162:1241–9. https://doi.org/10.1016/j.ijbiomac.2020.06.227.

[22] Chen JJ, Liang X, Li HX, et al. Improving the catalytic property of the glycoside hydrolase LXYL-P1–2 by directed evolution. Molecules 2017;22(12):2133. https://doi.org/10.3390/molecules22122133. PMid: 29207529.

[23] Rashid Z, Naeimi H, Zarnani AH, et al. Facile fabrication of nickel immobilized on magnetic nanoparticles as an efficient affinity adsorbent for purification of his-tagged protein. Mater Sci Eng C 2017;80(7):670–6. https://doi.org/10.1016/j.msec.2017.07.014. PMid: 28866214.

[24] Dyal A, Loos K, Noto M, et al. Activity of Candida rugosa lipase immobilized on γ-$Fe_2O_3$ magnetic nanoparticles. J Am Chem Soc 2003;125(7):1684–5. https://doi.org/10.1021/ja021223n. PMid: 12580578.

[25] Antony N, Balachandran S, Mohanan PV. Immobilization of diastase α-amylase on nano zinc oxide. Food Chem 2016;211(5):624–30. https://doi.org/10.1016/j.foodchem.2016.05.049. PMid: 27283676.

[26] Ling XM, Wang XY, Ma P, et al. Covalent immobilization of penicillin G acylase onto $Fe_3O_4$@ chitosan magnetic nanoparticles. J Microbiol Biotechnol 2016;26(5):829–36. https://doi.org/10.4014/jmb.1511.11052. PMid: 26869599.

[27] Xu LQ, Wen XH, Ding HJ. Immobilization of lignin peroxidase on spherical mesoporous material. Huanjing Kexue 2010;31(10):2493–9. https://doi.org/10.1631/jzus.A1000244. PMid: 21229767.

[28] Fang G, Chen H, Zhang Y, et al. Immobilization of pectinase onto $Fe_3O_4$@ $SiO_2$–$NH_2$ and its activity and stability. Int J Biol Macromol 2016;88(3):189–95. https://doi.org/10.1016/j.ijbiomac.2016.03.059. PMid: 27037054.

[29] Miller SR. An appraisal of the enzyme stability-activity trade-off. Evolution 2017;71(7):1876–87. https://doi.org/10.1111/evo.13275. PMid: 28542908.

[30] Turati FM, Júnior M, Wilson G, et al. Immobilization of lipase from Penicillium sp. section gracilenta (CBMAI 1583) on different hydrophobic supports: modulation of functional properties. Molecules 2017;22(2):339. https://doi.org/10.3390/molecules22020339. PMid: 28241445.

[31] Chen Y, Zhang Z, Jiang W, et al. RuIII@CMC/$Fe_3O_4$ hybrid: an efficient, magnetic, retrievable, self-organized nanocatalyst for green synthesis of pyranopyrazole and polyhydroquinoline derivatives. Mol Divers 2019;23:421–42. https://doi.org/10.1007/s11030-018-9887-3.

[32] Klapiszewski L, Zdarta J, Jesionowski T, et al. Titania/lignin hybrid materials as a novel support for alpha-amylase immobilization: a comprehensive study. Colloid Surf B Biointerfaces 2018;162:90–7. https://doi.org/10.1016/j.colsurfb.2017.11.045. PMid: 29169053.

[33] Landarani A, Taheri A, Amini M, et al. Xylanase immobilized on novel multifunctional hyperbranched polyglycerol-grafted magnetic nanoparticles: an efficient and robust biocatalyst. Langmuir 2015;31(33):9219–27. https://doi.org/10.1021/acs.langmuir.5b02004. PMid: 26258956.

[34] Zhang H, Hua SF, Li CQ, et al. Effect of graphene oxide with different morphological characteristics on properties of immobilized enzyme in the covalent method. Bioprocess Biosyst Eng 2020:1–12. https://doi.org/10.1007/s00449-020-02375-9.